


RESEARCH

Open Access



Multi-sensor tracking with partly overlapping FoV using detection field of probability modeling and the GLMB filter

Weifeng Liu^{1,2*} , Qiliang Liu¹, Yimei Chen² and Hailong Cui²

*Correspondence:
liuwf@sust.edu.cn

¹ School of Electrical and Control Engineering, Shaanxi University of Science and Technology, Xi'an, China

² School of Automation, Hangzhou Dian University, Hangzhou, China

Abstract

In this paper, we consider multi-sensor with partly overlapping field of view (FoV) in the labeled random finite set (L-RFS) framework. This is different from most existing multi-sensor tracking algorithms, where the sensors are assumed to have the same FoV. We describe the partly overlapping FoV by modeling probability field of detection for individual sensors in whole observation area and can be seen as the same range of FoV. We consider all these using generalized labeled multi-Bernoulli filter in labeled RFS framework. Besides, we also propose a measurement-driven target birth model. Finally, the effectiveness of the proposed algorithm is verified by experiments.

Keywords: Target tracking, Multi-sensor, Partly overlapping FoV, Labeled random finite sets, The GLMB filter

1 Introduction

The aim of target tracking of far distance using radar sensor is to infer the states of targets from a set of measurements, which are received by the sensor. It is widely used in the military field or civilian areas, where the single sensor has been studied a lots in current literatures, whether in association-based approaches such as joint probability data association [1, 2] and multiple hypothesis tracker [3], or in random finite sets-based approach. The RFS approach provides an elegant Bayesian formulation for multi-target tracking problem. The typical RFS multi-target tracking (RFS-MTT) filters include the probability hypothesis density (PHD) filter [4], Gaussian mixture (GM-PHD) filter [5], the cardinalized PHD (CPHD) filter [6, 7], and the (cardinality balanced) multi-Bernoulli (CBMeMber) filter [8, 9]. In multitarget tracking, a recent break-through is a closed form solution to the Bayes multitarget filter which can also output target tracks [10, 11]. The most important work is the generalized labeled multi-Bernoulli (GLMB) filter. It is with the first multitarget conjugate prior [10, 11] the multitarget conjugate prior with respect to the standard multitarget likelihood function, or Vo-Vo prior. Additionally, this multi-target prior is also closed under the Chapman-Kolmogorov equation for the standard multi-target transition density [10, 11].

The multi-sensor multi-target tracking has been studied a lots in traditional association-based algorithms. For example, the classic S-dimension assignment algorithm [12]. The multi-sensor with a distributed structure shows more robust performance than the centering one. Li et al. proposed the best linear unbiased estimator for the distributed sensors in reference[13]. This result can be used in the MSMT tracking. In the RFS framework, Mahler proposed multi-sensor PHD filter [4, 14, 15], all belonging to centralized structure and have the same measurement field. For the large range of target movement in the radar tracking network, it is difficult for a single radar to complete the tracking task. Reference [16] developed a collaborative detection and power allocation (CDPA) scheme, which can evidently expand the detection range and improve the target tracking accuracy. Further, the Bayesian Cramér-Rao lower bound (BCRLB) is used in [17, 18] to quantify the target tracking performance, and good results are obtained.

In fact, when a target flies thousands of kilometers, it is difficult for a sensor to track the target. Obviously, the assumption of multi-sensor having the same field is unrealistic. Usually, certain working pattern like relay race is adopt and thus the sensors are with partly overlapping field of view (FoV). At present, the basic idea to deal with this problem is to fuse the information in the overlapping FoV of each radar to improve the tracking performance, and to combine the information in the non-overlapping FoV to expand the sensing range. The main methods to solve this problem are dividing, clustering and other methods.

- Dividing method: References [19–21] used the known radar FoV to divide the multi-target density and then fused the divided terms to represent the multi-target density of overlapping FoV. However, the target information of non-overlapping FoV was ignored in [19].
- Clustering method: Using a clustering method, i.e., finding estimated matches from different sensors for the same target according to different measures, and performing fusion only on the selected matches. Reference [22] calculated the Mahalanobis distance between PHD Gaussian components of different sensors, and fused the Gaussian components with shorter Mahalanobis distance through the GA method, realizing the distributed GA fusion of PHD filters in partly overlapping FoV. Reference [23] achieved the fusion of CPHD filters in partly overlapping fields of view by using a method similar to that in [22]. Reference [24] matched the Bernoulli components between multi-Bernoulli filters through Mahalanobis distance and realized distributed AA fusion of multi-Bernoulli filters in limited FoV. For details about GA and AA fusion, see [25, 26]. Reference [27] used Optimal Subpattern Assignment (OSPA) distance as a measure to implement a method similar to that in [22]. Reference [28] used the method based on the highest a posteriori density distance measure to realize the PHD filter fusion of the limited FoV.
- Other methods: Reference [29] proposed a track-to-track fusion method in which the information contents of posteriors are combined. It is proved that using Cauchy Schwarz divergence can better realize LMB filter fusion with limited FoV. A distributed network of sensors with limited field of views is proposed under labeled RFS frameworks [27]. Reference [30] proposed a dual-term node-

wise separable likelihood. It can be used for cases in which the sensors have partly overlapping FoVs.

The target birth intensity (TBI) is widely assumed to have a constant amplitude that must be determined in advance, implying that the intensity of emerging targets will be the same in all FoV. However, this is not always desirable. In actual tracking scenarios, the size of TBI is usually unknown and changes over time [31–33]. In [34], the target birth probability is adaptively performed in the pre-processing step, combined with the current measurements to correct the preset of the target birth probability, the proposed filter can really adapt to the target birth situation and achieve better tracking accuracy. In [35], a magnitude-adaptive TBI approach has been developed for RFS-based Bayesian filters, which adapts the TBI magnitude online with respect to the newest observations in exchange for very little additional computation. Reference [36] modelled the time-varying spatial distribution of target births as a dynamic density map with adaptive grid points, which is capable of estimating the unknown, dynamically changing birth process.

In this paper, we model the partly overlapping detection field of probability and provide multi-sensor measurement driven birth model. Based on these, we adopt the labeled random finite set to describe the target states and estimate their states by using the generalized labeled multi-Bernoulli (GLMB) filter. The preliminary results of this paper are published in a conference version [37], and this article is a complete one.

The structure of this paper is organized as follows. The Sect. 2 shows some theoretical basis for the labeled random finite set, including the GLMB filter. The Sect. 3 proposes the models of the detection of probability for the sensors. Section 3 considers the multi-sensor GLMB filter with partly overlapping field. The simulation is given in Sect. 4, and Sect. 5 concludes this paper.

2 Background

2.1 The state and measurement RFSs

In category of RFS, the states and measurements of multi-target can be seen as a set, in which each element belongs to a random vector and the cardinality of the set is finite and random. More specifically, the multi-target state RFS can be modeled by [8]:

$$X_k = [\cup_{x \in X_{k-1}} S_{k|k-1}(x)] \cup [\cup_{x \in X_{k-1}} B_{k|k-1}(x)] \cup \Gamma_k \quad (1)$$

where $S_{k|k-1}(x)$, $B_{k|k-1}(x)$, and Γ_k are the target surviving, spawned, and birth RFSs. Let these RFSs are mutually independent. Then, the probability density of the multi-target state RFS can be gotten by [8]:

$$f_{k|k-1}(X_k|X_{k-1}) = \sum_{W \subseteq X_k} \pi_{T,k|k-1}(W|X_{k-1}) \pi_{\Gamma,k}(X_k - W) \quad (2)$$

where $T_{k|k-1}(x) \triangleq S_{k|k-1}(x) \cup B_{k|k-1}(x)$, $\pi_{\Gamma,k}(\cdot)$ is the probability densities of spontaneous birth RFS Γ_k . The equation describes all actions of target motion, birth and death. It should be noted that the spawning case is ignored in the paper.

The multi-target is observed by various sensors and multiple measurements may be received. Assume at time k , a target may be detected and produces a measurement z_k with probability $P_D(x_k)$ or missed and gives empty set $\{\emptyset\}$ with probability $1 - P_D(x_k)$.

In a word, the received measurements z_k , with probability of detection $P_D(x_k)$ and likelihood function $g(z_k|x_k)$, involve all the information of the target state RFS X_k . The target measurement RFS plus clutter or false alarms RFS K_k are expressed in the following:

$$Z_k = \Theta_k(X_k) \cup K_k \quad (3)$$

where $\Theta_k(X_k) = \cup_{x_k \in X_k} \Theta_k(x_k)$, we may model $\Theta_k(x_k)$ as a binary RFS

$$\Theta_k(x_k) = \begin{cases} \emptyset, & \text{with probability } 1 - P_D(x_k) \\ \{z_k\}, & \text{with probability } P_D(x_k) \end{cases}$$

The K_k is Poisson RFS with intensity $\nu_K(\cdot)$. Its probability distribution is derived by:

$$c_k(z_k) = \nu_{K,k}(z_k) / \int \nu_{K,k}(z_k) dz_k \quad (4)$$

Under the assumption of mutual independence between $\Theta_k(X_k)$ and K_k , the probability density $\varphi_k(Z_k|X_k)$ is given by [8]:

$$\varphi_k(Z_k|X_k) = \sum_{W \subseteq Z_k} \pi_{\Theta_k}(W|X_k) \pi(Z_k - W) \quad (5)$$

where $\pi_{\Theta_k}(W|X_k)$ is the probability density of target-generated measurement RFS and $\pi(Z_k - W)$ for clutter.

2.2 The labeled random finite set

Based on traditional RFS, a variable of label is added to the above state element x [10], generated a labeled RFS. It is defined on a product space $\mathbb{X} \times \mathbb{L}$, where \mathbb{L} is a label space. In practical applications, a labeled random vector is represented by a unique vector in a discrete countable space. For example, the label is defined on space $(k, i)^T$, where k is time stamp and i is the count of this stamp. Some densities of the labeled RFS version are shown in the following.

2.2.1 The labeled Poisson RFS

A Poisson distribution is defined on the positive integer space $N \triangleq \{0, 1, \dots, n, \dots\}$ and given by

$$\pi(x = n) = \frac{\lambda^n e^{-\lambda}}{n!} \quad (6)$$

where λ is Poisson intensity. For a RFS $X = \{x_1, \dots, x_n\}$, the elements $x_i \in X$ are i.i.d with density $\nu(x)/\bar{N}$, where $\bar{N} = \int \nu(x) dx$. Its Poisson distribution is given by

$$\pi(x = n) = \frac{\lambda^n e^{-\lambda}}{n!} \quad (7)$$

where λ is Poisson intensity. For a RFS $X = \{x_1, \dots, x_n\}$, the elements $x_i \in X$ are i.i.d with density $\nu(x)/\bar{N}$, where $\bar{N} = \int \nu(x) dx$. Its Poisson distribution is given by

$$\pi(\{x_1, \dots, x_n\}) = e^{\tilde{N}} \prod_{i=1}^n v(x_i) \quad (8)$$

A labeled Poisson RFS X is expressed by $X = \{(x_1, \ell_1), \dots, (x_n, \ell_n)\}$ with the following density function:

$$\pi(\{(x_1, \ell_1), \dots, (x_n, \ell_n)\}) = \delta_{L(n)}(\{\ell_1, \dots, \ell_n\}) \text{Pois}_{\langle v, 1 \rangle}(n) \prod_{i=1}^n \frac{v(x_i)}{\langle v, 1 \rangle} \quad (9)$$

where $\delta_{L(n)}(\{\ell_1, \dots, \ell_n\})$ is a generalization of the Kronecker delta

$$\delta_Y(X) = \begin{cases} 1, & \text{if } X = Y \\ 0, & \text{otherwise} \end{cases}$$

$\langle v, 1 \rangle$ is defined to be $\int v(x) dx$, $\text{Pois}_{\langle v, 1 \rangle}(n)$ is the Poisson distribution, i.e., $e^{-\lambda} \lambda^n / n!$, $\lambda = \langle v, 1 \rangle$.

2.2.2 Labeled multi-Bernoulli RFS

For a fixed number of independent Bernoulli RFS $X^{(i)}$ with parameters of existing probability $r^{(i)}$ and density $p^{(i)}(\cdot)$, their union

$$X = \cup_{i=1}^n X^{(i)} \quad (10)$$

belongs to a multi-Bernoulli RFS and with the following probability density

$$\pi(\{x_1, \dots, x_n\}) = \prod_{j=1}^N (1 - r^{(j)}) \sum_{1 \leq i_1 \neq \dots \neq i_n \leq N} \prod_{l=1}^n \frac{r^{(i_l)} p^{(i_l)}(x_l)}{1 - r^{(i_l)}} \quad (11)$$

For a labeled multi-Bernoulli RFS X with non-empty parameter set $\{r^{(\zeta)}, p^{(\zeta)}, \zeta \in \Psi\}$, its probability distribution is given by [38]

$$\begin{aligned} \pi(\{(x_1, \ell_1), \dots, (x_n, \ell_n)\}) &= \delta_n(|\{\ell_1, \dots, \ell_n\}|) \\ &\times \prod_{\zeta \in \Psi} (1 - r^{(\zeta)}) \prod_{j=1}^n \frac{1_{\alpha(\Psi)}(\ell_j) r^{(\alpha^{-1}(\ell_j))} p^{(\alpha^{-1}(\ell_j))}(x_j)}{1 - r^{(\alpha^{-1}(\ell_j))}} \end{aligned} \quad (12)$$

where function $\alpha(\cdot)$ is a 1-1 map shown as: $\alpha: \Psi \rightarrow \mathbb{L}$. It should be noted that the distribution is not a multi-Bernoulli distribution. For simplicity, an alternative form of the labeled multi-Bernoulli distribution is given by [10]:

$$\pi(X) = \Delta(X) 1_{\alpha(\Psi)}(\mathcal{L}(X)) [\Phi(X; \cdot)]^\Psi \quad (13)$$

where $\Delta(X)$ is an indicator function to guarantee the distinct of individual labels. $\Phi(X; \cdot)$ is defined by

$$\Phi(X; \cdot) = \begin{cases} 1 - r^{(\zeta)}, & \text{if } \alpha(\zeta) \notin \mathcal{L}(X) \\ r^{(\zeta)} p^{(\zeta)}(x), & \text{if } (x, \alpha(x)) \in X \end{cases}$$

2.2.3 Generalized labeled multi-Bernoulli density

The generalized labeled multi-Bernoulli density is defined by [10]

$$\pi(X) = \Delta(X) \sum_{c \in \mathbb{C}} \omega^{(c)}(\mathcal{L}(X)) [p^{(c)}]^X \quad (14)$$

where c is a discrete index set, $\omega^{(c)}$ is a weighted coefficient and dependent on the state label $\mathcal{L}(X)$. $p^{(c)} \triangleq p^{(c)}(x, \ell)$ is a distribution function for track with label ℓ . Thus, the exponential function $[p^{(c)}]^X$ is the factorial of all tracks. Moreover, it has been shown that the labeled Poisson RFS and labeled multi-Bernoulli are two special cases of GLMB RFSs [10].

3 Methods

3.1 The measurement models

Let $F_{s,k}$ be the observation area for the sensor s . That is, only the targets in the field $F_{s,k}$ may be observed. Assume that the state of sensor s is $y_{s,k} \in R^{n_y}$, where R^{n_y} is the n_y -dimensional Euclidean space. The measurement model can be modeled by:

$$Z_{s,k} = \cup_{x_k \in X_k} \Theta_{s,k}(x_k, y_{s,k}) \cup K_{s,k}(y_{s,k}) \quad (15)$$

The measurement model for sensor s is given by:

$$\Theta_k^s(y_{s,k}, x_k) = \begin{cases} \{z_{s,k}\} & \text{with } P_d(y_{s,k}, x_k), \text{ if } \mathcal{P}(x_k) \in F_{s,k} \\ \emptyset & \text{with } 1 - P_d(y_{s,k}, x_k) \text{ otherwise} \end{cases}$$

where $\mathcal{P}(\cdot)$ is a projection from certain state space R^{n_x} to position space R^2 , i.e., $\mathcal{P} : R^{n_x} \rightarrow R^2$ for target state.

3.2 The models of multi-sensor probability of detection

In general, radar is a feasible sensor for tracking targets over long distances. Its field of view can be regarded as a fan-shaped area in polar coordinates, as shown in Fig. 1. It is defined by:

$$A_{s,k} : [\theta_{s,\min}(y_{s,k}), \theta_{s,\max}(y_{s,k})] \times [0, r_s(y_{s,k})] \subseteq [-\pi, \pi] \times \mathbb{R}^+ \quad (16)$$

where $A_{s,k}$ is the FoV of the sensor s , \mathbb{R}^+ is the space of positive real numbers. Accordingly, the corresponding Euclidean space position can be gotten by a projection $q : A_{s,k} \rightarrow R^2$. Thus, the FoV area in Euclidean space is defined by $F_{s,k} = \{q(a_{s,k}) \mid \text{for all } a_{s,k} \in A_{s,k}\}$. The model of probability of detection for sensor s is given by

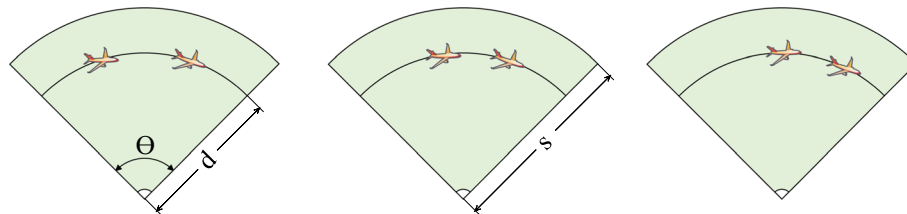


Fig. 1 Multi-sensor observations

$$P_{s,d}(x_k) = \begin{cases} P_D \exp \left\{ -\frac{\|\mathcal{P}(x_k) - \mathcal{P}(y_{s,k})\|_2}{2} \right\}, & \text{if } \mathcal{P}(x_k) \in F_{s,k} \\ 0, & \text{otherwise} \end{cases}$$

where P_D is a constant, $\|\cdot\|_2$ is 2-norm. This model implies that a target may be detected with a certain probability if it locates in area $F_{s,k}$ of sensor s , and with probability of detection zero otherwise.

3.3 Target birth models of multi-sensor measurement driven

In most existing algorithms, the FoV of a sensor is assumed to cover all the track region and there is no any dead zone. Hence, the target birth model is assumed to be prior and known. But for sensors with partly overlapping FoV, a sensor scans only part of the surveillance region. Hence, it is impossible to detect a target when the target is born outside the FoV. In order to build the target birth model, we refer the measurement-driven birth model given in [38–40] and extend it to the multi-sensor case.

A multi-Bernoulli RFS X is a union of a fixed number of independent Bernoulli RFSs $X^{(i)}$ with existence probability $r_B^{(i)} \in (0, 1)$ and probability density $p_B^{(i)} (i = 1, \dots, M)$ [41]. So, the probability density of a multi-Bernoulli RFS can be abbreviated as:

$$\pi = \left\{ (r_B^{(i)}, p_B^{(i)}) \right\}_{i=1}^M \quad (17)$$

Assume that the form of the birth model with generalized labeled multi-Bernoulli (GLMB) is as follows:

$$\pi_B(\mathbf{X}_+) = \Delta(\mathbf{X}_+) w_B(\mathcal{L}(\mathbf{X}_+)) [p_B]^{\mathbf{X}_+} \quad (18)$$

where

$$w_B(I) = \prod_{i \in \mathbb{B}} (1 - r_B^{(i)}) \prod_{l \in I} \frac{1_{\mathbb{B}}(l) r_B^{(l)}}{1 - r_B^{(l)}} \quad (19)$$

The existence probability can be initialized by the following equation:

$$r_B(z_k^1, \dots, z_k^S) = \min \left(r_{B \max}, \prod_s \frac{\lambda_B^s r_U(z_k^1, \dots, z_k^S)}{\sum_{(\zeta_k^1, \dots, \zeta_k^S) \in Z_k^1 \times \dots \times Z_k^S} r_U(\zeta_k^1, \dots, \zeta_k^S)} \right) \quad (20)$$

where

$$r_U(z_k^1, \dots, z_k^S) = 1 - \sum_{(I, \xi) \in \mathcal{F}(\mathbb{L}) \times \Xi} \sum_{\vartheta \in \Theta(I, S)} 1_{z_\theta}(z) w^{(I, \xi, \vartheta)} \quad (21)$$

where $\Theta(I, S)$ is the space of multi-sensor association map. ϑ is a multi-sensor association map (defined next subsection).

3.4 Multi-sensor association map

In the GLMB filter, the association map plays a crucial role in the RFS multi-objective likelihood function.

Definition 1 [10]: The association map is a mapping: $\theta: \mathbb{L} \rightarrow \{0, 1, \dots, |Z|\}$. If $\theta(i) = \theta(i') > 0$, it means $i = i'$, the set Θ represents the associated map space, and its subset I can be represented by $\Theta(I)$. The association diagram describes the correspondence between the trajectory and the measurement, the trajectory l produces a measure of $z_{\theta(l)} \in Z$, and the undetected trajectory is denoted by 0.

Definition 2 [42]: The multi-sensor association map is a mapping: $\vartheta: \mathbb{L} \rightarrow S_1 \times S_2 \times \dots \times S_m$, $S_s = \{0, 1, \dots, |Z_s|\}$, where $\vartheta(i) = \vartheta(i')$, $\theta(i, l) \neq 0$ means $i = i'$, $\theta(i, l)$ is the r th element in vector $\theta(i)$. The set $\Theta(I, S)$ represents the space of multi-sensor associated map, and its subset I can be represented by $\Theta(I, S)$.

Under the independence of all sensors, the multi-sensor association map ϑ can be expressed as

$$\vartheta \triangleq (\vartheta_1^T, \dots, \vartheta_S^T) \quad (22)$$

where ϑ_s^T can be seen as components of ϑ . Assume that multi-sensor measurements can be represented by $Z_k \triangleq Z_{1,k} \cup \dots \cup Z_{S,k}$, multi-sensor posterior probability:

$$f(X_k|Z_k) = \frac{g(Z_k|X_k)f(X_k)}{\int g(Z_k|X_k)f(X_k)\delta X_k} \quad (23)$$

where the integral is defined as:

$$\int f(X_k)\delta X_k = \sum_{i=0}^{\infty} \frac{1}{i!} \sum_{(l_1, \dots, l_i) \in \mathbb{L}^i} \int f(\{(x_1, l_1), \dots, (x_i, l_i)\}) d(x_1, \dots, x_i) \quad (24)$$

Assume that the multi-sensor are independent, then multi-sensor likelihood function is given by:

$$g(Z_k|X_k) = \prod_{s=1}^S e^{-\langle K_s, 1 \rangle} K_s^{Z_{s,k}} \sum_{\vartheta_s \in \Theta(\mathcal{L}(X), S)} [\psi_{Z_{s,k}}(\cdot; \vartheta_s)]^X \quad (25)$$

where

$$\psi_{Z_{s,k}}(x, l; \vartheta_s) = \begin{cases} \frac{P_{s,d}(x, l)g(z_{\vartheta_s(l)}|x, l)}{k(z_{\vartheta_s(l)})}, & \text{if } \vartheta_s(l) > 0 \\ 1 - P_{s,d}(x, l), & \text{if } \vartheta_s(l) = 0 \end{cases} \quad (26)$$

3.5 GLMB estimation algorithm for multi-sensor with partly overlapping FoV

The basic principle of the multi-sensor tracking algorithm is to distribute the multi-sensor reasonably. At different times, the detection results of the individual sensors may be different. At each moment, we need to judge the target, to determine the target in which the sensor within the scope of observation. The specific multi-sensor GLMB estimation algorithm is as follows:

3.5.1 Update step

If the multi-sensor multi-target a priori density function is the form of generalized labeled multi-Bernoulli, then the multi-sensor multi-target posterior probability density is also the form of generalized labeled multi-Bernoulli:

$$\pi(\mathbf{X}_k | Z_k) = \Delta(\mathbf{X}_k) \sum_{(I, \xi) \in \mathcal{F}(\mathbb{L}) \times \Xi} \sum_{\vartheta \in \Theta(I, S)} w^{(I, \xi, \vartheta)}(Z_k) \times \delta_I(\mathcal{L}(\mathbf{X}_k)) \left[p^{(\xi, \vartheta)}(\cdot | Z_k) \right]^{\mathbf{X}_k} \quad (27)$$

where ϑ represents the current multi-sensor association map. The association parameters are defined as follows:

$$\begin{aligned} w^{(I, \xi, \vartheta)}(Z_k) &= \frac{\delta_{\vartheta-1}(\{\prod_{s=1}^S \{0: |Z_{s,k}| \}\}) (I) w^{(I, \xi)} \left[\eta_{Z_k}^{(\xi, \vartheta)} \right]^I}{\sum_{(I, \xi) \in \mathcal{F}(\mathbb{L}) \times \Xi} \sum_{\vartheta \in \Theta(I, S)} \delta_{\vartheta-1}(\{\{0: |Z_k|\}\}) (I) w^{(I, \xi)} \left[\eta_{Z_k}^{(\xi, \vartheta)} \right]^I} \\ p^{(\xi, \vartheta)}(x, l | Z_k) &= \frac{p^{(\xi)}(x, l) \psi_{Z_k}(x, l; \vartheta)}{\eta_{Z_k}^{(\xi, \vartheta)}(l)} \\ \eta_{Z_k}^{(\xi, \vartheta)}(l) &= \langle p^{(\xi)}(\cdot, l), \psi_{Z_k}(\cdot, l; \vartheta) \rangle \\ \psi_{Z_k}(x, l; \vartheta) &= \delta_0(\vartheta(l)) q_D(x, l) + (1 - \delta_0(\vartheta_s(l))) \frac{\prod_{s=1}^S P_{s,d}(x, l) g(z_{\vartheta_s(l)} | x, l)}{\prod_{s=1}^S K(z_{\vartheta_s(l)})} \end{aligned} \quad (28)$$

where $\psi_{Z_k}(x, l; \vartheta)$ is the likelihood function in the case of multi-sensor; assume that the sensors are independent of each other, it can be simplified as: $\prod \psi_{Z_{1,k}} \cdots \psi_{Z_{S,k}}(\cdot; \vartheta_s)$, suppose that the likelihood function is a Gaussian distribution, $P_{s,d}(x_k, l) = P_{s,d}$, $g(z_{s,k} | x_k, l) = \mathcal{N}(z_{s,k}; H_{s,k}, R_{s,k})$. $H_{s,d}$ and $R_{s,d}$ are the observation matrix and measurement noise covariance for sensor s . Assume that probability density $p^{(\xi)}(\cdot, \ell)$ of target ℓ follows a Gaussian mixture distribution:

$$p^{(\xi)}(\cdot, \ell) = \sum_{i=1}^{J^{(\xi)}(\ell)} w_i^{(\xi)}(\ell, 0) \mathcal{N}(x; \mu_i^{(\xi)}(\ell, 0), P_i^{(\xi)}(\ell, 0)) \quad (29)$$

Then we can get the following multi-sensor cost matrix:

$$C_{i,S} = -Ln \left[\frac{\prod_{s=1}^S P_{s,d} \sum_{j=1}^{J^{(\xi)}(l_i)} q_k^{(\xi)}(z_{k,j}^s; l_i)}{\prod_{s=1}^S (1 - P_{s,d}) K(z_k^s)} \right] \quad (30)$$

where $z_{k,j}^s$ represents the j th measurement of the s th sensor, the update history (ξ, ϑ) and $\eta_{Z,k}^{(\xi, \vartheta)}$ of the multi-sensor association map are as follows:

$$\eta_{Z_k}^{(\xi, \vartheta)} = \prod_{s=1}^S \sum_{i=1}^{J^{(\xi, s)}(\ell)} w_{z_{k,i}^s}^{(\xi, \vartheta_s)}(\ell) \quad (31)$$

$$p^{(\xi, \vartheta)}(x_k, \ell | Z_k) = \prod_{s=1}^S \sum_{i=1}^{J^{(\xi, s)}(\ell)} \frac{w_{z_{k,j}^s}^{(\xi, \vartheta_s)}(\ell)}{\eta_{Z_k}^{(\xi, \vartheta)}} \mathcal{N}(x; \mu_{z_{k,j}^s}^{(\xi, \vartheta_s)}(\ell), P_i^{(\xi, \vartheta_s)}(\ell)) \quad (32)$$

Although the multi-sensor labeled multi-Bernoulli filter has the same representation as the single-sensor, there are many differences between the multi-sensor and the single-sensor for the specific parameters:

$$w_{Z_k^s, i}^{(\xi, \vartheta_s)}(\ell) = w_{Z_k^s, i}^{(\xi, \vartheta)}(\ell, j-1) \times \begin{cases} \frac{P_{D,s} q_i^{(\xi, \vartheta_s)}(z_{\vartheta_s}(\ell, j); \ell)}{\kappa(z_{\vartheta_s}(\ell, j))}, & \text{if } \vartheta_s(\ell, j) > 0 \\ 1 - P_{D,s}, & \text{if } \vartheta_s(\ell, j) = 0 \end{cases} \quad (33)$$

$$\begin{aligned} q_i^{(\xi, \vartheta_s)}(z_{\vartheta_s}(\ell, j); \ell) &= \mathcal{N}(z_{k,j}^s; H_{k,s} \mu_{Z_k^s, i}^{(\xi, \vartheta_s)}(\ell, m-1), H_{k,s} P_i^{(\xi, \vartheta_s)}(\ell, j-1) H_{k,s}^T + R_{k,s}) \\ \mu_{Z_k^s, i}^{(\xi, \vartheta_s)}(\ell) &= \begin{cases} \mu_{Z, i}^{(\xi, \vartheta)}(\ell, j-1) + K_i^{(\xi, \vartheta_s)} \\ \times (z_{\vartheta}(\ell, j) - H_{k,s} \mu_{Z_k^s, i}^{(\xi, \vartheta_s)}(\ell, j-1)) H_{k,s}^T, & \text{if } \vartheta_s(\ell, j) > 0 \\ \mu_{Z_k^s, i}^{(\xi, \vartheta_s)}(\ell, j-1), & \text{if } \vartheta_s(\ell, j) = 0 \end{cases} \\ K_i^{(\xi, \vartheta_s)}(\ell) &= \begin{cases} P_i^{(\xi, \vartheta_s)}(\ell, j-1) H_{k,s}^T (H_{k,s} P_i^{(\xi, \vartheta_s)}(\ell, j-1) H_{k,s}^T)^{-1}, & \text{if } \vartheta_s(\ell, j) > 0 \\ 0, & \text{if } \vartheta_s(\ell, j) = 0 \end{cases} \end{aligned} \quad (34)$$

The above formula gives the recursive process of the measurement Z_1 to Z_m of the multi-sensor association map.

3.5.2 Predict step

The predict step is the same as the case of single sensor. That is, if the multi-sensor multi-target a priori density function is the form of the generalized labeled multi-Bernoulli, then the multi-objective prediction is:

$$\pi_+(X_+) = \Delta(X_+) \sum_{(I_+, \xi) \in \mathcal{F}(\mathbb{L}) \times \Xi} w_+^{(I_+, \xi)} \delta_{I_+}(\mathcal{L}(X_+)) \left[p_+^{(\xi)} \right]^{X_+} \quad (35)$$

where

$$\begin{aligned} w_+^{(I_+, \xi)} &= w_B(I_+ \cap \mathbb{B}) w_s^{(\xi)}(I_+ \cap \mathbb{L}) \\ p_+^{(\xi)}(x, l) &= 1_{\mathbb{L}}(l) p_s^{(\xi)}(x, l) + (1 - 1_{\mathbb{L}}(l)) p_B(x, l) \\ p_s^{(\xi)}(x, l) &= \frac{\langle p_s(\cdot, l) f(x|\cdot, l), p^{(\xi)}(\cdot, l) \rangle}{\eta_s^{(\xi)}(l)} \\ \eta_s^{(\xi)}(l) &= \int \langle p_s(\cdot, l) f(x|\cdot, l), p^{(\xi)}(\cdot, l) \rangle dx \\ w_s^{(\xi)}(L) &= \left[\eta_s^{(\xi)} \right]^L \sum_{I \in L} 1_I(L) [q_s^{(\xi)}]^{I-L} w^{(I, \xi)} \\ q_s^{(\xi)}(l) &= \left\langle q_s(\cdot, l), p_s^{(\xi)}(\cdot, l) \right\rangle \end{aligned} \quad (36)$$

In this step, the multi-sensor has the same form as the single-sensor. Let $w_B(I_+ \cap \mathbb{B})$ be the weight of new label $I_+ \cap \mathbb{B}$, $w_s^{(\xi)}(I_+ \cap \mathbb{L})$ is the weight of the survival label $(I_+ \cap \mathbb{L})$, $p_B(x, l)$ is the probability density of the new target. $p_s^{(\xi)}(x, l)$ is the density of the survival target obtained from the prior density $p^{(\xi)}(\cdot, l)$. $f(x|\cdot, l)$ represents the probability density of the survival target.

Algorithm 1 provides pseudocode for a multi-sensor multi-target tracking algorithm with partly overlapping fields of view.

Algorithm 1 Multi-sensor multi-target tracking algorithm with partly overlapping fields of view

Input: Measurements $Z_k^{1 \dots S}$, Times K , The number S and FoV of sensors

Output: The number, states and trajectories of multi-target

```

1: for  $k = 1 : K$  do
2:   Initialize target birth model parameters.
3:   for  $j = 1 : S$  do
4:     Prediction multi-target density  $\pi_{k|k-1}$ , see Eq (35).
5:     Obtain measurements of multi-target  $Z_k^j$ , see Sec. 3.1.
6:     Update birth target model parameters, see Sec. 3.3.
7:     Update multi-target density  $\pi_{k|k}$ , see Eq (27).
8:     Obtain number, states and trajectories of multi-target.
9:   end for
10:  Merge:  $X_k = \bigcup x_{k,i}$ 
11: end for

```

4 Experiments and discussions

To verify the effectiveness and robustness of the proposed algorithm, we set up two scenarios. Experiment 1: high detection probability and small number of targets; Experiment 2: low detection probability and a larger number of targets. As the number of targets increases, more targets are born or die out outside the radar field of view, which poses a challenge to the trajectory tracking capability of the proposed algorithm. The reduction in detection probability also has a direct impact on tracking accuracy.

4.1 Experiment 1: high detection rate scenario and tracking a small number of targets

Given three sensors located in positions $y_k^1 = [200 \text{ km}, 0 \text{ km}]'$, $y_k^2 = [500 \text{ km}, 0 \text{ km}]'$, $y_k^3 = [800 \text{ km}, 0 \text{ km}]'$, respectively. The surveillance sectors are all $[\pi/6, 5\pi/6] \times [0, 100] \text{ rad} \cdot \text{km}$ for the sensors. This means that the range of angle is 120° , detection probability $P_D = 0.98$, survival probability $P_s = 0.99$, clutter intensity $\lambda_c = 3$. Assume the running steps is 200. Consider three targets move in $x - y$ coordinate. The targets move in a constant velocity (CV) model, i.e.,

$$x_{k+1,i} = Ax_{k,i} + v_{k,i} \quad (37)$$

where the transfer matrix A is:

$$A = \begin{bmatrix} 1 & T & 0 & 0 \\ 0 & 1 & 0 & 0 \\ 0 & 0 & 1 & T \\ 0 & 0 & 0 & 1 \end{bmatrix} \quad (38)$$

where sampling time $T = 1$, let state $x_k^i = [p_{k,x}; \dot{p}_{k,x}; p_{k,y}; \dot{p}_{k,y}]$ represent the positions and velocities in x and y directions, respectively. The observation function is angle and range.

$$z_{k,i}^s = [\sqrt{(p_{k,x}^i - u_{k,x}^s)^2 + (p_{k,y}^i - u_{k,y}^s)^2}, \arctan \frac{p_{k,y}^i - u_{k,y}^s}{p_{k,x}^i - u_{k,x}^s}]' + w_k^s \quad (39)$$

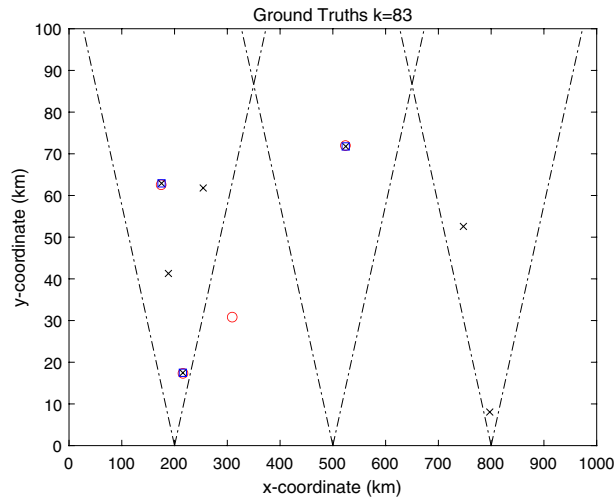


Fig. 2 The fields for the four sensors

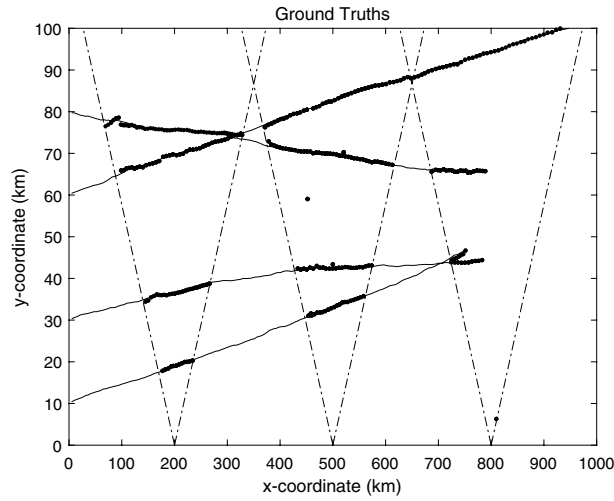


Fig. 3 Ground truths vs. estimated tracks

where $y_k^s \triangleq [u_{k,x}^s, u_{k,y}^s]^T$ is the position of sensor s . The surviving time interval for target 1 is $[1, 150]$ s, for target 2 is $[30, 170]$ s, and for target 3 and target 4 is $[50, 200]$ s. The initial states of the four targets are listed in the following:

$$\begin{aligned} x_0^1 &= [0 \text{ km}, 5 \text{ km/s}, 80 \text{ km}, -0.15 \text{ km/s}]^T, & x_0^2 &= [0 \text{ km}, 5 \text{ km/s}, 30 \text{ km}, 0.15 \text{ km/s}]^T \\ x_0^3 &= [0 \text{ km}, 7 \text{ km/s}, 60 \text{ km}, 0.15 \text{ km/s}]^T, & x_0^4 &= [0 \text{ km}, 5 \text{ km/s}, 10 \text{ km}, 0.2 \text{ km/s}]^T \end{aligned}$$

Only when a target enters into the surveillance region of a sensor. It can be observed. The fields of the four sensors are shown in Fig. 2.

From the figure, the fan-shaped areas are shown by two dashed lines and three fixed sensors with partly overlapping fields. Only a target entering into a sensor's field can be observed.

The target tracks are given in Fig. 3. It can be seen that the initial flying heights in y coordinate are 80 km, 30 km, 60 km and 10 km, respectively. The target 1 enters the

observation range of the first sensor 1 around $k = 20$. After moving about 250 km distance, the target 1 moves out of the field of sensor 1 and the measurement cannot be derived simultaneously. About 400 km on the horizontal axis, the first target enters into the observation range of sensor 2 and is observed. Also after around 600 km, target 1 moves out of the field of sensor 2. At about 700 km on the horizontal axis, it enters the observation range of sensor 3 and is observed until it dies within the field of sensor 3. Targets 2 and 3 have the same fields. It can be seen from the figure the proposed algorithm can detect and track the three targets correctly in each sensor field.

Figure 4 shows the trajectories of the targets in the x, y directions and the total flight times are 200s. The time intervals of all target births and deaths are $[1, 150]$ s, $[30, 170]$ s, $[50, 200]$ s, $[50, 200]$ s for targets 1 to 4, respectively. Considering the partly overlapping FoV, it can be seen from the figure the whole tracking process well. Each target is detected in various time intervals. For example, in time interval around $[10, 65]$ s, target 1 lies in the FoV of sensor 1. And in time interval $[75, 110]$ s target 1 lies in the FoV of sensor 2 and in time interval $[130, 150]$ s of sensor 3. It can be seen from this figure that the proposed algorithm can successfully detect the targets by using the multi-sensor measurement driven birth model.

The estimation of the number of targets is shown in the upper sub-figure of Fig. 5, where the true number of targets and its estimated value are plotted. It can be seen from Fig. 5 the three targets do not enter into the observation region of all three sensors at the first 20th time steps, so the estimated number of targets is 0. Once target 1 enters into the region, the estimated number of targets becomes 1. In practice, in certain time interval if a target is not detected, it means that the target locates in the

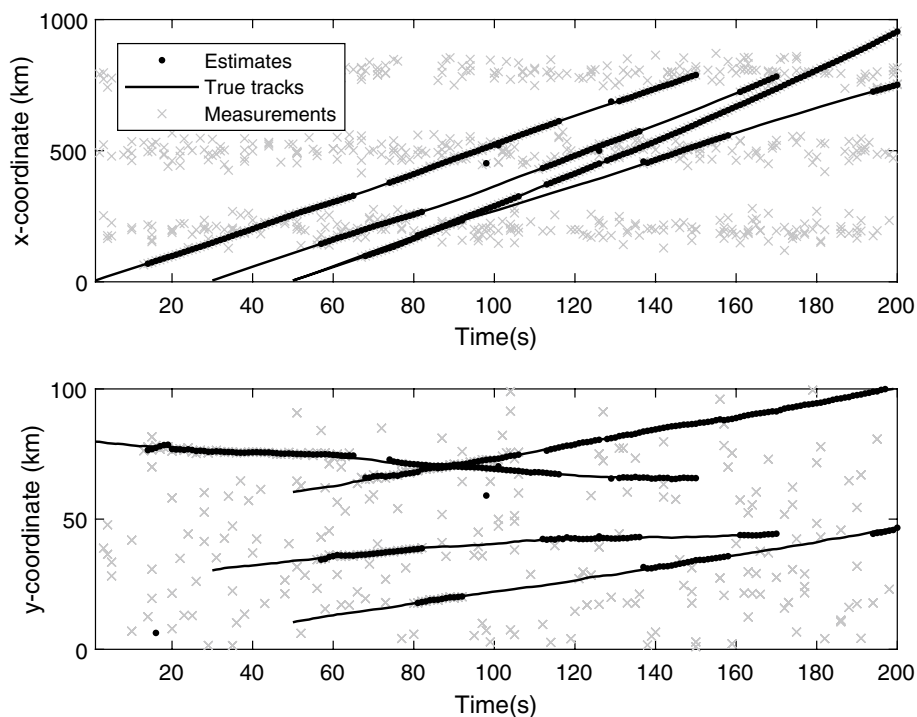


Fig. 4 The true tracks vs. estimated tracks in x, y directions

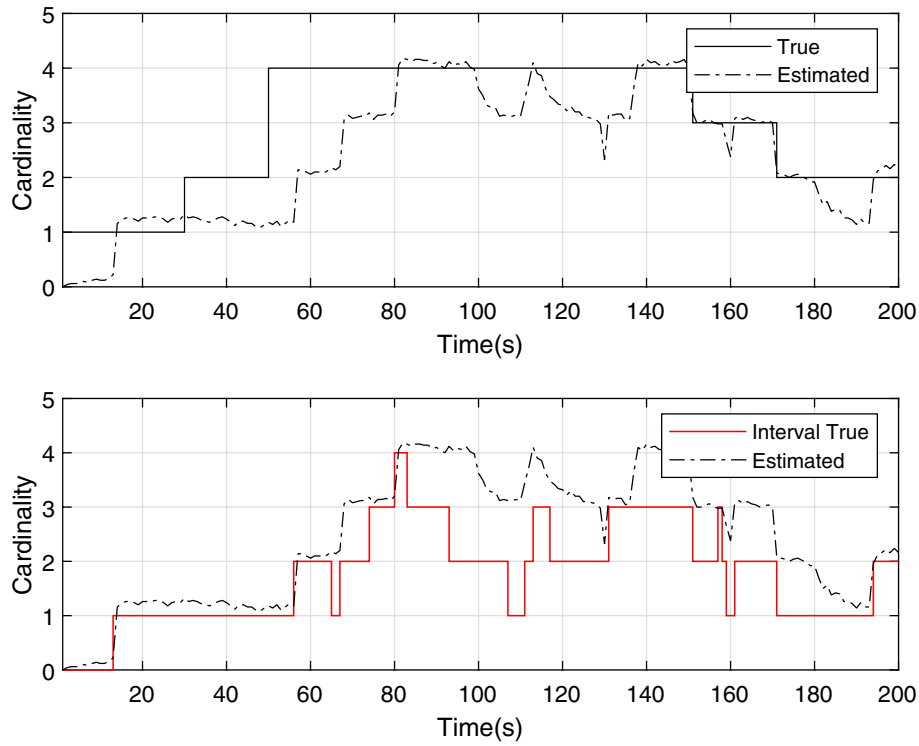


Fig. 5 The estimation of the number of targets

blind region or has been died. Therefore, the estimated number of targets and the true value are not coincident in this time interval. Only in the observation region, the target can be detected. Outside the field, nothing can be found. Therefore, it is meaningful to get the true number of detected targets in the observation region, which is plotted in the bottom sub-figure of Fig. 5. It can be seen from the sub-figure that the number of targets can be estimated efficiently.

Here we use the optimal subpattern assignment (OSPA) metric to evaluate the tracking performance [43]:

$$OSPA(p, c, X, \hat{X}) = \left[\frac{1}{n} \left(\min_{\pi \in \Pi_n} \sum_{i=1}^n d(c, x_i, \hat{x}_{\pi(i)})^p + c^p (m - n) \right) \right]^{1/p}, n \leq m \quad (40)$$

$$OSPA(p, c, X, \hat{X}) = OSPA(p, c, \hat{X}, X), n > m \quad (41)$$

$$OSPA(\infty, c, X, \hat{X}) = \begin{cases} \min_{\pi \in \Pi_n} \max_{1 \leq i \leq n} d(c, x_i, \hat{x}_{\pi(i)}) & m = n \\ c & m \neq n \end{cases} \quad (42)$$

The parameters $c = 50, p = 1$ and the OSPA error is shown in Fig. 6. It shows that the OSPA error, OSPA location error and cardinality error, respectively. It seems there is a large error. In fact, if considering the detected region (outside blind area), the corresponding OSPA error given in Fig. 7 is much better. This shows that in the observation

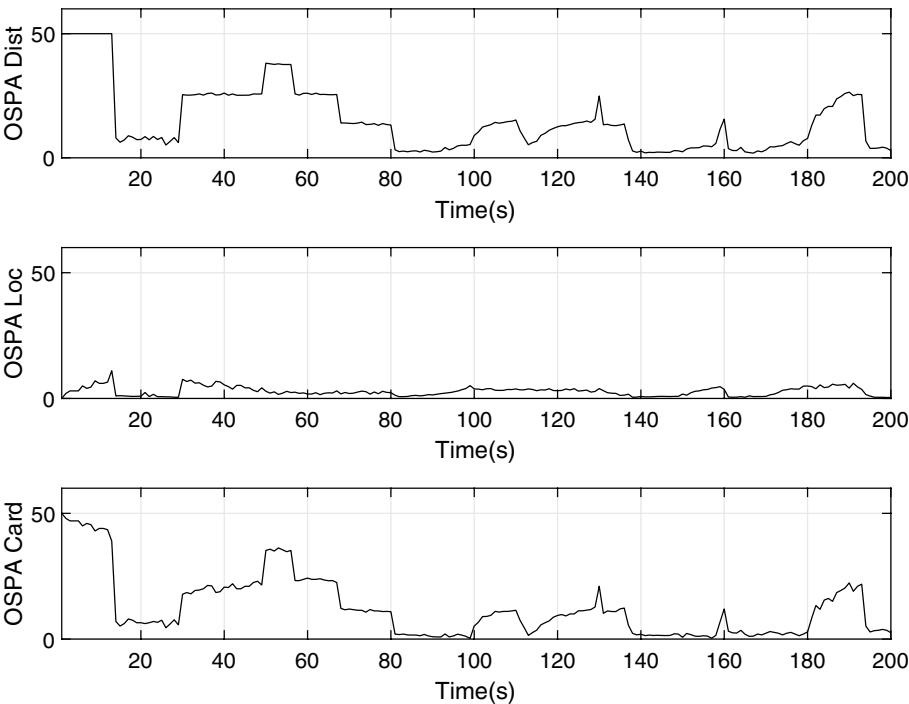


Fig. 6 The OSPA error (50MCs) with considering the blind area

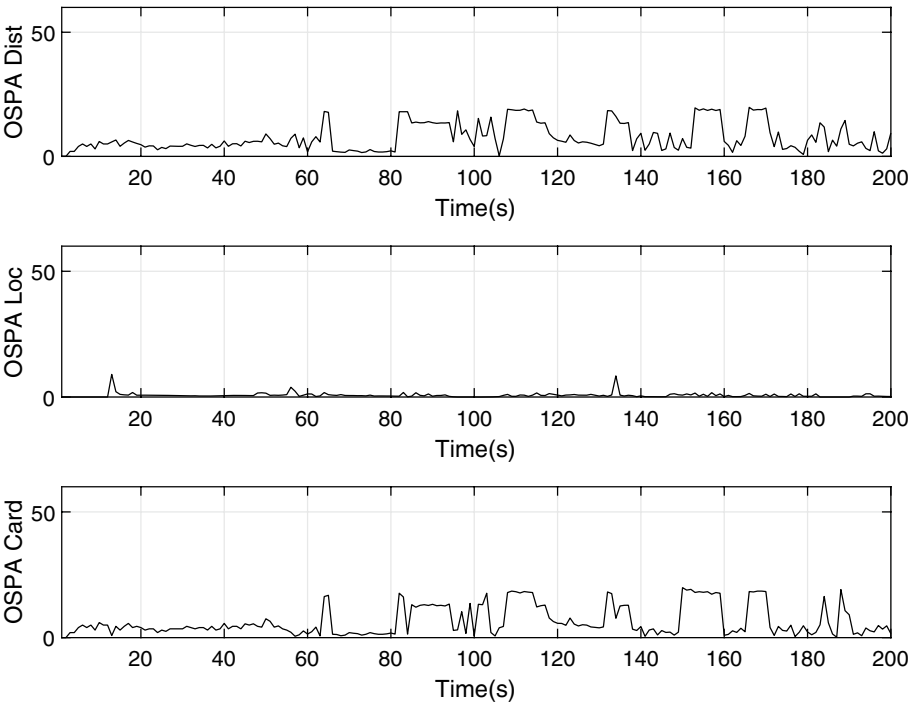


Fig. 7 The OSPA error (50MCs). Only considering the detected area

area of all sensors, the targets are detected and tracked well and the number of targets is accurately estimated.

4.2 Experiment 2: low detection rate scenario and tracking more targets

In this scenario, we will verify that the proposed algorithm can correctly track a large number of targets under more complex low detection probability conditions. The initial position of the sensor and other parameters remains unchanged; only the detection probability of each sensor is modified to 0.80. At the same time, we increase the number of targets to 10, whose motion model is still the CV model. The initial state and survival time of these targets are given by:

$$\begin{aligned} x_0^1 &= [0 \text{ km}, 5 \text{ km/s}, 90 \text{ km}, -0.05 \text{ km/s}]^T, & T_{\text{birth}} &= 1 \text{ s}, & T_{\text{death}} &= 150 \text{ s} \\ x_0^2 &= [0 \text{ km}, 5 \text{ km/s}, 10 \text{ km}, 0.1 \text{ km/s}]^T, & T_{\text{birth}} &= 1 \text{ s}, & T_{\text{death}} &= 200 \text{ s} \\ x_0^3 &= [0 \text{ km}, 5 \text{ km/s}, 90 \text{ km}, -0.2 \text{ km/s}]^T, & T_{\text{birth}} &= 1 \text{ s}, & T_{\text{death}} &= 150 \text{ s} \\ x_0^4 &= [0 \text{ km}, 5 \text{ km/s}, 10 \text{ km}, 0.2 \text{ km/s}]^T, & T_{\text{birth}} &= 30 \text{ s}, & T_{\text{death}} &= 200 \text{ s} \\ x_0^5 &= [0 \text{ km}, 5 \text{ km/s}, 40 \text{ km}, -0.2 \text{ km/s}]^T, & T_{\text{birth}} &= 30 \text{ s}, & T_{\text{death}} &= 200 \text{ s} \\ x_0^6 &= [0 \text{ km}, 5 \text{ km/s}, 40 \text{ km}, 0.01 \text{ km/s}]^T, & T_{\text{birth}} &= 50 \text{ s}, & T_{\text{death}} &= 200 \text{ s} \\ x_0^7 &= [0 \text{ km}, 5 \text{ km/s}, 40 \text{ km}, 0.2 \text{ km/s}]^T, & T_{\text{birth}} &= 50 \text{ s}, & T_{\text{death}} &= 200 \text{ s} \\ x_0^8 &= [0 \text{ km}, 5 \text{ km/s}, 70 \text{ km}, 0.2 \text{ km/s}]^T, & T_{\text{birth}} &= 70 \text{ s}, & T_{\text{death}} &= 200 \text{ s} \\ x_0^9 &= [0 \text{ km}, 5 \text{ km/s}, 70 \text{ km}, -0.2 \text{ km/s}]^T, & T_{\text{birth}} &= 70 \text{ s}, & T_{\text{death}} &= 200 \text{ s} \\ x_0^{10} &= [0 \text{ km}, 5 \text{ km/s}, 70 \text{ km}, 0.01 \text{ km/s}]^T, & T_{\text{birth}} &= 70 \text{ s}, & T_{\text{death}} &= 200 \text{ s} \end{aligned}$$

The tracks for 10 targets are given in Fig. 8. As can be seen from the figure, the initial flight altitude of the target is 90 km, 70 km, 40 km and 10 km. Throughout the 200 s of tracking, the position estimate of target was fairly accurate. It shows that even in the case of low detection probability, the algorithm proposed in this paper can still track a large number of targets correctly. However, in Figs. 8 and 9, we can find that when the target enters the field of view of the sensor, especially when multiple targets overlap, there will be a comparatively large error in the position estimation. At low detection probability, when multi-target are in close proximity, the measurements obtained by the sensors are incomplete and the relative positions of these measurements are very close

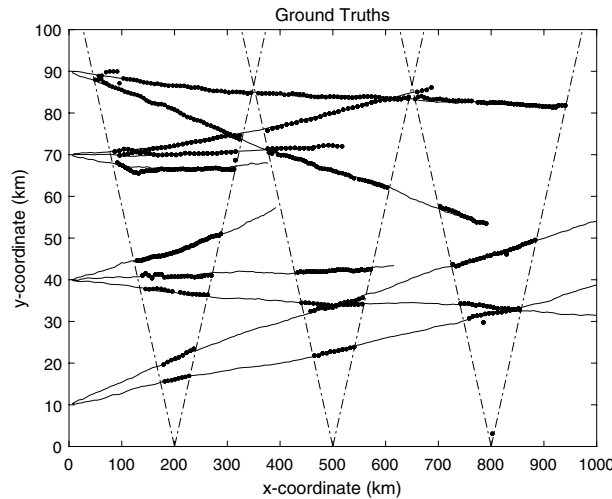


Fig. 8 Ground truths vs. estimated tracks(10 targets)

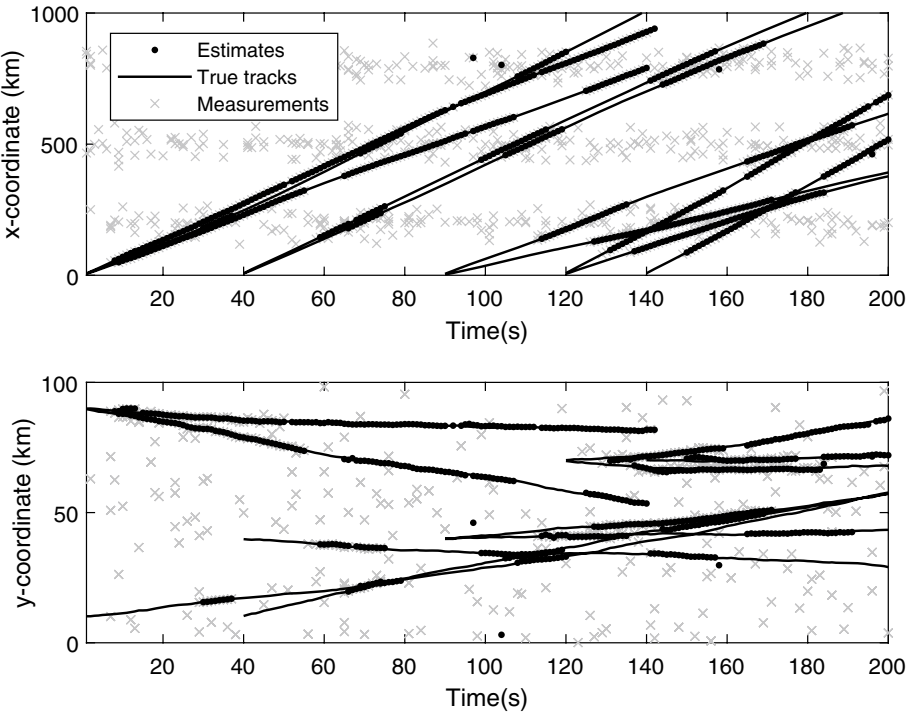


Fig. 9 The true tracks vs. estimated tracks in x, y directions(10 targets)

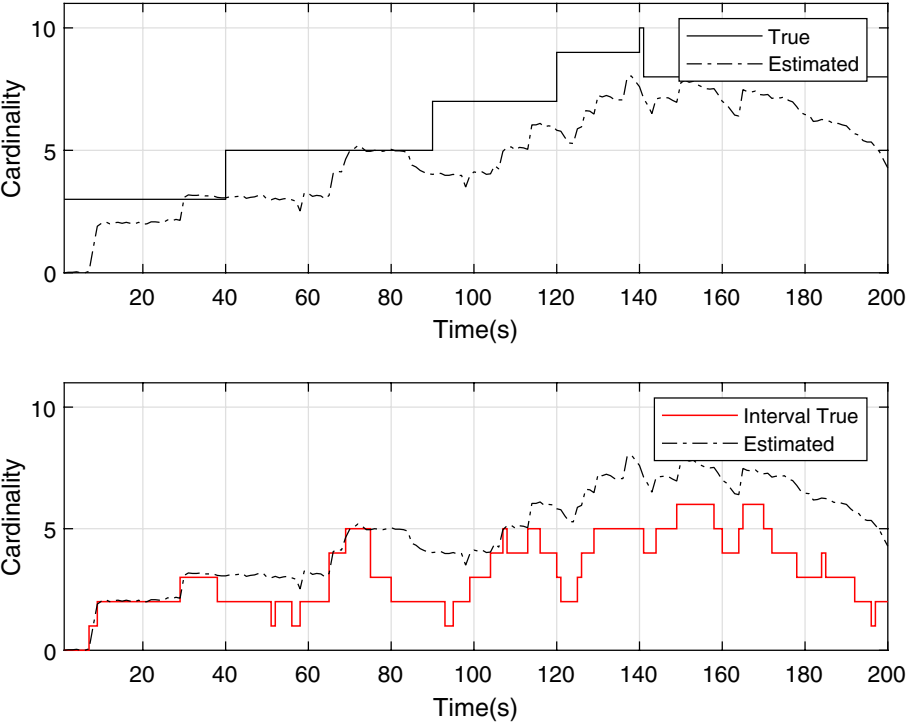


Fig. 10 The estimation of the number of targets

together. This will pose a great challenge to the filter update process. And this is often seen in sensor tracking with limited field of view.

Similar to Scenario 1, the estimated number of 10 targets is given in Fig. 10. Targets can only be correctly estimated when they appear in the sensor field of view. For example, between 1 and 40 s, 3 targets actually survive. But it was not until about the 10th second that two targets entered the field of view of Sensor 1. A third target enters the field of view of Sensor 1 around the 30th second. By this time, the number of targets detected by the sensor is 3.

The OSPA error of target location estimation at low detection probability is given in Fig. 11. The parameters $c = 50, p = 1$. When the blind area is considered, the OSPA error of the position estimation is larger. But when the blind area is not considered, as shown in Fig. 12, the OSPA error, OSPA position error and OSPA cardinality error are quite small. This illustrates that in scenarios with low detection probability, the target can be well tracked when it is within the field of view of the sensor and can be satisfied with practical tracking tasks.

5 Conclusions

In this paper, we consider the target tracking problem of multi-sensor partly overlapping FoV. We establish a model to describe partly overlapping FoV using probability field of detection (PFoD). Then, a multi-sensor multi-target tracking algorithm based on generalized labeled multi-Bernoulli (GLMB) filter is proposed. Finally, the proposed algorithm is verified by using three sensors with partly overlapping fields. Experiments show that the effective of the algorithm in detecting and tracking multi-target.

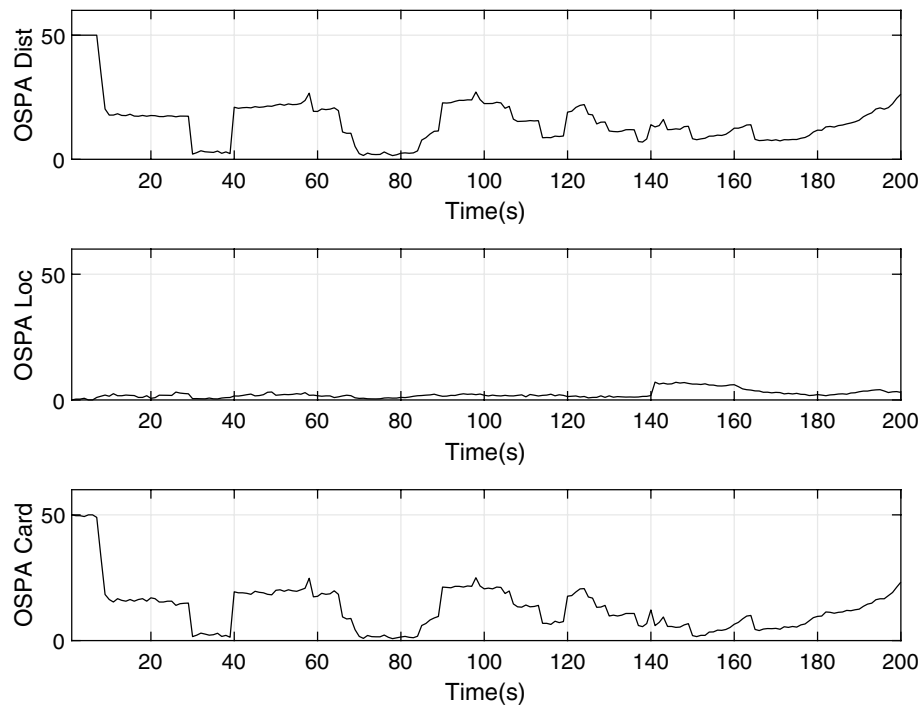


Fig. 11 The OSPA error (50MCs) with considering the blind area

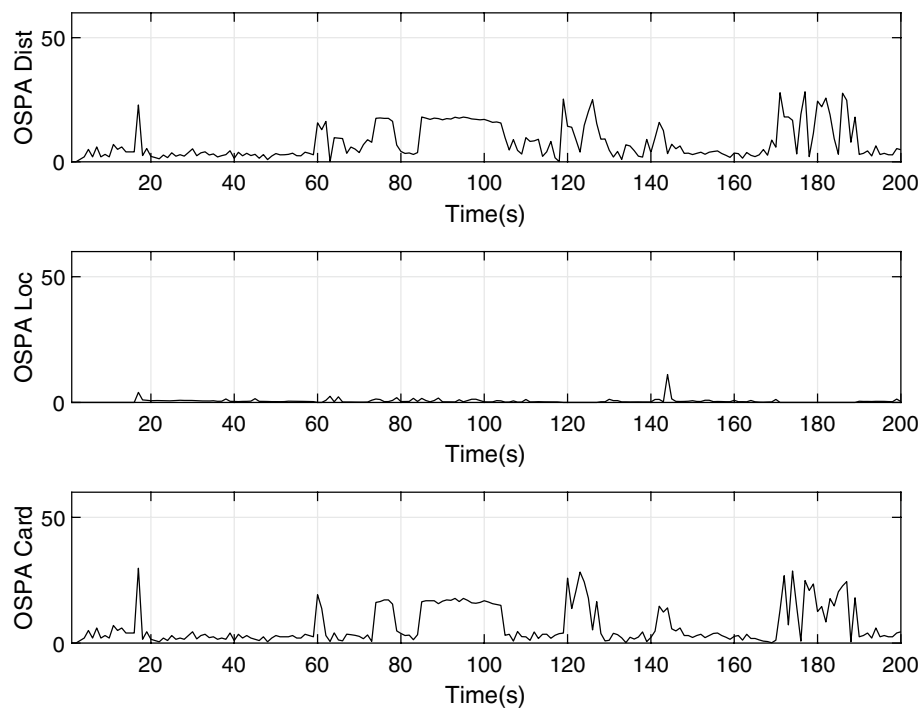


Fig. 12 The OSPA error (50MCs). Only considering the detected area

Abbreviations

FoV	Field of view
RFS	Random finite set
L-RFS	Labeled random finite set
PFoD	Probability field of detection
GLMB	Generalized labeled multi-Bernoulli
PHD	Probability hypothesis density
CPHD	Cardinalized PHD
CBMeMber	Cardinality balanced multi-target multi-Bernoulli
GM-PHD	Gaussian mixture probability hypothesis density
KNN	K-nearest neighbor algorithm
CV model	Constant velocity model
OSPA	Optimal sub-pattern assignment

Acknowledgements

Not applicable.

Author contributions

WL developed and wrote the method presented in this paper. QL and JY performed the experiments. All authors discussed the results and implications and commented on the manuscript at all stages. All authors read and approved the final manuscript.

Funding

This work was supported in part by the NSFC(61771177), and the key research and development program of Shaanxi province (2021GY-087)

Availability of data and materials

In this work, we have used the free RFS MATLAB code provided by Prof. Ba-Ngu Vo and Prof. Ba-Tuong Vo at <http://ba-tuong.vo-au.com/codes.html>.

Declarations

Ethics approval and consent to participate

Not applicable.

Consent for publication

Not applicable.

Competing interests

The authors declare that they have no competing interests.

Received: 15 June 2022 Accepted: 15 December 2022

Published online: 04 January 2023

References

1. Y. Bar-Shalom, Tracking methods in a multitarget environment. *IEEE Trans. Autom. Control* **23**(4), 618–626 (1978)
2. Y. Bar-Shalom, T.E. Fortmann, P.G. Cable, Tracking and data association. *Acoust. Soc. Am. J.* **87**(2), 918–919 (1990)
3. D. Reid, An algorithm for tracking multiple targets. *IEEE Trans. Autom. Control* **24**(6), 843–854 (1979)
4. R.P. Mahler, Multitarget bayes filtering via first-order multitarget moments. *IEEE Trans. Aerosp. Electron. Syst.* **39**(4), 1152–1178 (2003)
5. B.-N. Vo, W.-K. Ma, The gaussian mixture probability hypothesis density filter. *IEEE Trans. Signal Process.* **54**(11), 4091–4104 (2006)
6. R. Mahler, Phd filters of higher order in target number. *IEEE Trans. Aerosp. Electron. Syst.* **43**(4), 1523–1543 (2007)
7. B.-T. Vo, B.-N. Vo, A. Cantoni, Analytic implementations of the cardinalized probability hypothesis density filter. *IEEE Trans. Signal Process.* **55**(7), 3553–3567 (2007)
8. R.P. Mahler, Statistical Multisource-multitarget Information Fusion, *Artech House Norwood* (MA, USA, 2007)
9. B.-T. Vo, B.-N. Vo, A. Cantoni, The cardinality balanced multi-target multi-bernoulli filter and its implementations. *IEEE Trans. Signal Process.* **57**(2), 409–423 (2008)
10. B.-T. Vo, B.-N. Vo, Labeled random finite sets and multi-object conjugate priors. *IEEE Trans. Signal Process.* **61**(13), 3460–3475 (2013)
11. B.-N. Vo, B.-T. Vo, D. Phung, Labeled random finite sets and the bayes multi-target tracking filter. *IEEE Trans. Signal Process.* **62**(24), 6554–6567 (2014)
12. S. Deb, M. Yeddanapudi, K. Pattipati, Y. Bar-Shalom, A generalized sd assignment algorithm for multisensor-multitarget state estimation. *IEEE Trans. Aerosp. Electron. Syst.* **33**(2), 523–538 (1997)
13. X.R. Li, Y. Zhu, J. Wang, C. Han, Optimal linear estimation fusion. i. unified fusion rules. *IEEE Trans. Inf. Theory* **49**(9), 2192–2208 (2003)
14. R. Mahler, The multisensor phd filter: I. general solution via multitarget calculus, in *Signal Processing, Sensor Fusion, and Target Recognition XVIII* (International Society for Optics and Photonics, 2009), vol. 7336, p. 73360
15. R. Mahler, Approximate multisensor cphd and phd filter, in *2010 13th International Conference on Information Fusion* (IEEE, 2010), pp. 1–8
16. J. Yan, W. Pu, S. Zhou, H. Liu, Z. Bao, Collaborative detection and power allocation framework for target tracking in multiple radar system. *Inf. Fusion* **55**, 173–183 (2020)
17. J. Yan, W. Pu, S. Zhou, H. Liu, M.S. Greco, Optimal resource allocation for asynchronous multiple targets tracking in heterogeneous radar networks. *IEEE Trans. Signal Process.* **68**, 4055–4068 (2020)
18. J. Yan, J. Dai, W. Pu, H. Liu, M. Greco, Target capacity based resource optimization for multiple target tracking in radar network. *IEEE Trans. Signal Process.* **69**, 2410–2421 (2021)
19. T. Li, V. Elvira, H. Fan, J.M. Corchado, Local-diffusion-based distributed smc-phd filtering using sensors with limited sensing range. *IEEE Sens. J.* **19**(4), 1580–1589 (2018)
20. K. Da, T. Li, Y. Zhu, Q. Fu, Gaussian mixture particle jump-markov-cphd fusion for multitarget tracking using sensors with limited views. *IEEE Trans. Signal Inf. Process. Netw.* **6**, 605–616 (2020)
21. L. Gao, G. Battistelli, L. Chisci, Fusion of labeled rfs densities with different fields of view. *IEEE Trans. Aerospace Electron. Syst.* 1–16 (2022)
22. M. Vasic, D. Mansolino, A. Martinoli, A system implementation and evaluation of a cooperative fusion and tracking algorithm based on a gaussian mixture phd filter, in *2016 IEEE/RSJ International Conference on Intelligent Robots and Systems (IROS)* (IEEE, 2016), pp. 4172–4179
23. G. Li, G. Battistelli, L. Chisci, W. Yi, L. Kong, Distributed multi-view multi-target tracking based on cphd filtering. *Signal Process.* **188**, 108210 (2021)
24. S. Wu, L. Wang, T. Li, Multi-bernoulli target tracking based on distributed limited sensing network. *Acta Automatica Sinica* **48**(5), 1370–1384 (2022)
25. K. Da, T. Li, Y. Zhu, H. Fan, Q. Fu, Recent advances in multisensor multitarget tracking using random finite set. *Front. Inf. Technol. Electron. Eng.* **22**(1), 5–24 (2021)
26. Y. Cao, O. Kaiwartya, T. Li, *Secure and Digitalized Future Mobility: Shaping the Ground and Air Vehicles Cooperation* (CRC Press, 2022)
27. H. Van Nguyen, H. Rezatofighi, B.-N. Vo, D.C. Ranasinghe, Distributed multi-object tracking under limited field of view sensors. *IEEE Trans. Signal Process.* **69**, 5329–5344 (2021)
28. W. Yi, G. Li, G. Battistelli, Distributed multi-sensor fusion of phd filters with different sensor fields of view. *IEEE Trans. Signal Process.* **68**, 5204–5218 (2020)
29. A.K. Gostar, T. Rathnayake, R. Tennakoon, A. Bab-Hadiashar, G. Battistelli, L. Chisci, R. Hoseinnezhad, Cooperative sensor fusion in centralized sensor networks using cauchy-schwarz divergence. *Signal Process.* **167**, 107278 (2020)
30. M. Üney, B. Mulgrew, D. Clark, Distributed localisation of sensors with partially overlapping field-of-views in fusion networks, in *2016 19th International Conference on Information Fusion (FUSION)* (IEEE, 2016), pp. 1340–1347
31. L. Chai, L. Kong, S. Li, W. Yi, The multiple model multi-bernoulli filter based track-before-detect using a likelihood based adaptive birth distribution. *Signal Process.* **171**, 107501 (2020)
32. C. Berry, D.J. Bucci, S.W. Schmidt, Passive multi-target tracking using the adaptive birth intensity phd filter, in *2018 21st International Conference on Information Fusion (FUSION)* (IEEE, 2018), pp. 353–360

33. Q. Huang, L. Xie, H. Su, Estimations of time-varying birth cardinality distribution and birth intensity in gaussian mixture cphd filter for multi-target tracking. *Signal Process.* **190**, 108321 (2022)
34. X. Hu, H. Ji, L. Liu, Adaptive target birth intensity multi-bernoulli filter with noise-based threshold. *Sensors* **19**(5), 1120 (2019)
35. T. Li, S. Sun, J.M. Corchado, M.F. Siyau, Random finite set-based bayesian filters using magnitude-adaptive target birth intensity, in *17th International Conference on Information Fusion (FUSION)* (IEEE, 2014), pp. 1–8
36. Q. Huang, L. Xie, X. Hu, H. Su, Kernel-based learning of birth process from evolving spatiotemporal rfs data stream in smccphd filter for multi-target tracking. *Signal Process.* **203**, 108783 (2023)
37. W. Liu, Y. Chen, H. Cui, Q. Ge, Multi-sensor tracking with on-overlapping field for the glmb filter, in *The Sixth International Conference on Control, Automation and Information Sciences (ICCAIS 2017)* (IEEE, 2017), pp. 202–207
38. S. Reuter, B.-T. Vo, B.-N. Vo, K. Dietmayer, The labeled multi-bernoulli filter. *IEEE Trans. Signal Process.* **62**(12), 3246–3260 (2014)
39. B. Ristic, D. Clark, B.-N. Vo, B.-T. Vo, Adaptive target birth intensity for phd and cphd filters. *IEEE Trans. Aerosp. Electron. Syst.* **48**(2), 1656–1668 (2012)
40. S. Lin, B.T. Vo, S.E. Nordholm, Measurement driven birth model for the generalized labeled multi-bernoulli filter, in *2016 International Conference on Control, Automation and Information Sciences (ICCAIS)* (IEEE, 2016), pp. 94–99
41. B.-T. Vo, B.-N. Vo, A. Cantoni, The cardinality balanced multi-target multi-bernoulli filter and its implementations. *IEEE Trans. Signal Process.* **57**(2), 409–423 (2009)
42. W. Liu, B. Wei, S. Zhu, A multi-sensor generalized labeled multi-bernoulli filter via extended association map, in *2015 International Conference on Control, Automation and Information Sciences (ICCAIS)* (IEEE, 2015), pp. 225–230
43. D. Schuhmacher, B.-T. Vo, B.-N. Vo, A consistent metric for performance evaluation of multi-object filters. *IEEE Trans. Signal Process.* **56**(8), 3447–3457 (2008)

Publisher's Note

Springer Nature remains neutral with regard to jurisdictional claims in published maps and institutional affiliations.

Submit your manuscript to a SpringerOpen[®] journal and benefit from:

- Convenient online submission
- Rigorous peer review
- Open access: articles freely available online
- High visibility within the field
- Retaining the copyright to your article

Submit your next manuscript at ► [springeropen.com](https://www.springeropen.com)
